PROCEEDINGS OF SCIENCE

Chandra X-ray observations of the HII region G5.89−0.39 and TeV Source HESSJ1800−240B

Gavin Rowell[1], Dieter Horns[2], Yasunobu Uchiyama[3], Stefan Funk[3], Stefan Wagner[4], Brent Nicholas[1], and H.E.S.S. Collaboration[5]

1. *School of Chemistry & Physics, University of Adelaide, Adelaide, Australia*
2. *Institut für Experimental Physik, Universität Hamburg, D22761 Hamburg, Germany*
3. *Kavli Institute for Particle Physics and Cosmology, Stanford, CA-94025, USA*
4. *Landessternwarte, Universität Heidelberg, Königstuhl D69117 Heidelberg, Germany*
5. *http://www.mpi-hd.mpg.de/hfm/HESS/*

E-mail: growell@physics.adelaide.edu.au

The TeV gamma-ray sources in the field of the old age ($> 10^4$ yr) supernova remnant (SNR) W28 [2] present a unique opportunity to probe for a new type of multi-TeV particle accelerator, namely, HII regions. One such example is the TeV source HESS J1800−240B which is found towards the highly unusual HII region complex G5.89−0.39. In this context X-rays studies are highly valuable in probing the particle acceleration potential of such HII regions and their subsequent contribution to the gamma-ray emission. Previous high resolution *XMM-Newton* X-ray observations despite being affected by stray light from a nearby X-ray binary, revealed several sources co-located with the two star forming components of G5.89−0.39, namely G5.89-0.39A, a HII region, as well as G5.89-0.39B, an ultracompact or UCHII region. Here we describe preliminary analysis and results from our *Chandra* observations towards G5.89−0.39 and HESS J1800−240B (∼80 ks) which are not affected by stray light. With *Chandra*, we reveal over 200 X-ray sources which appear to cluster somewhat towards G5.89−0.39A and B respectively. This includes possibly extended emission towards a massive O5 or earlier spectral type star (known as Feldt's star) thought to provide much of the ionisation and energetics in G5.89−0.39B. Some of the X-ray sources exhibit energetics typical of young moderate to high mass stars. Our *Chandra* observations reveal for the first time the extent of star formation in the two HII components. Ongoing work centres on detailed spectral studies, cross-correlation with stellar catalogues, and the search for extended X-ray emission.

25th Texas Symposium on Relativistic Astrophysics - TEXAS 2010
December 06-10, 2010
Heidelberg, Germany

PoS(Texas 2010)187

1. Introduction and Motivation

Observations >0.1 TeV with H.E.S.S. (High Energy Stereoscopic System) have revealed TeV (10^{12} eV) γ-ray sources in the field of the W28 (G6.4−0.1) supernova remnant (SNR) [3] (distance $d \sim 2-3$ kpc). W28 is a mixed morphology SNR $\sim 50'$ in diameter with shell-like radio continuum and centre-filled X-ray emission, and age between 35 and 150 kyr (see e.g. [22, 7] and references therein).

The four TeV sources towards the W28 SNR are notable for several reasons: (1) They represent only the second example, after the Galactic Ridge central molecular zone (CMZ) [2], where a very clear spatial match between TeV emission and molecular gas is noticed. Such a match is generally good evidence in favour of a hadronic origin for the multi-TeV accelerated particles; (2) The north-eastern TeV emission (HESS J1801−233) is situated where the W28 SNR shock is known to be interacting with a molecular cloud (based on 1720 MHz OH masers and shocked gas measurements indicating disruption from the W28 side of the cloud; see e.g. [9, 5, 18]). In this case, W28 is likely the source of accelerated particles in this region; (3) The TeV emission complex towards the south of W28 comprises three components. The brightest components are situated towards HII regions, and in particular the central TeV portion, HESS J1801−240B, is well centred on the unusual HII complex G5.89−0.39 which is thought to have a distance $d \sim 2$ kpc.

G5.89−0.39 itself comprises two components, a conventional HII region G5.89−0.39A and an ultra-compact (UC) HII region G5.89−0.39B several arcminutes to the west [14]. G5.89−0.39B exhibits arcminute-scale energetic ($> 10^{46}$ erg over few$\times$1000 yr) bi-polar molecular outflows [1, 23], which are surrounded by dense ($n \sim 10^5$ cm^{-3}) molecular gas. The blue and red-shifted outflows of about one arcminute length each have peaks separated by about $8''$ and appear to be aligned generally along our line of sight [27]. Continuum observations [8] (875 μm and 3.6 cm) reveal a $5''$ diameter shell which is likely blown out by a the winds of a massive protostar, possibly an O5 (or earlier) star identified as Feldt's star (T 40000K; Mass >200M$_\odot$) offset from the shell centre [11, 21]. The dense gas is observed up to arcminute scales (e.g. [23, 15, 27]), with distinct peaks centred on the G5.89−0.39A and B components [14, 18]. Strong infrared emission (particularly at 8μm) is centered on G5.89−0.39A and B with a striking infrared ring feature $\sim 10'$ wide (see Fig. 1 right panel) centred on G5.89−0.39A, perhaps powered by the strong stellar winds from this more evolved component. Fig. 1 summarises the various multiwavelength views (radio, infrared, dense molecular gas, TeV gamma-rays) with emphasis on the G5.89−0.39/HESSJ1800−240B region.

The key question we aim to address with *Chandra* is whether or not G5.89−0.39 contributes to the particle acceleration and TeV gamma-ray emission in HESS J1800−240B. Particles accelerated to TeV energies would produce non-thermal X-ray synchrotron photons, with related TeV emission coming from inverse-Compton scattering. The arcsec angular resolution of *Chandra* allows it to map X-ray emission on < 0.02 pc scales in G5.89−0.39, potentially resolving many features within the HII regions such as the $5''$ diameter radio shell as well as the molecular outflows. The radio/IR shell may represent a termination shock as stellar wind particles interact with the star's natal molecular cloud. Such situations have been discussed as plausible sites to accelerate particles to TeV energies (e.g. [4, 6]). In general the observation of any non-thermal X-ray emission from HII regions would also have major implications for our understanding of particle acceleration to multi-TeV energies in our Galaxy. To-date, only middle to latter stellar evolution phases (e.g.

massive stars, SNRs, and neutron star environments) are associated with such acceleration.

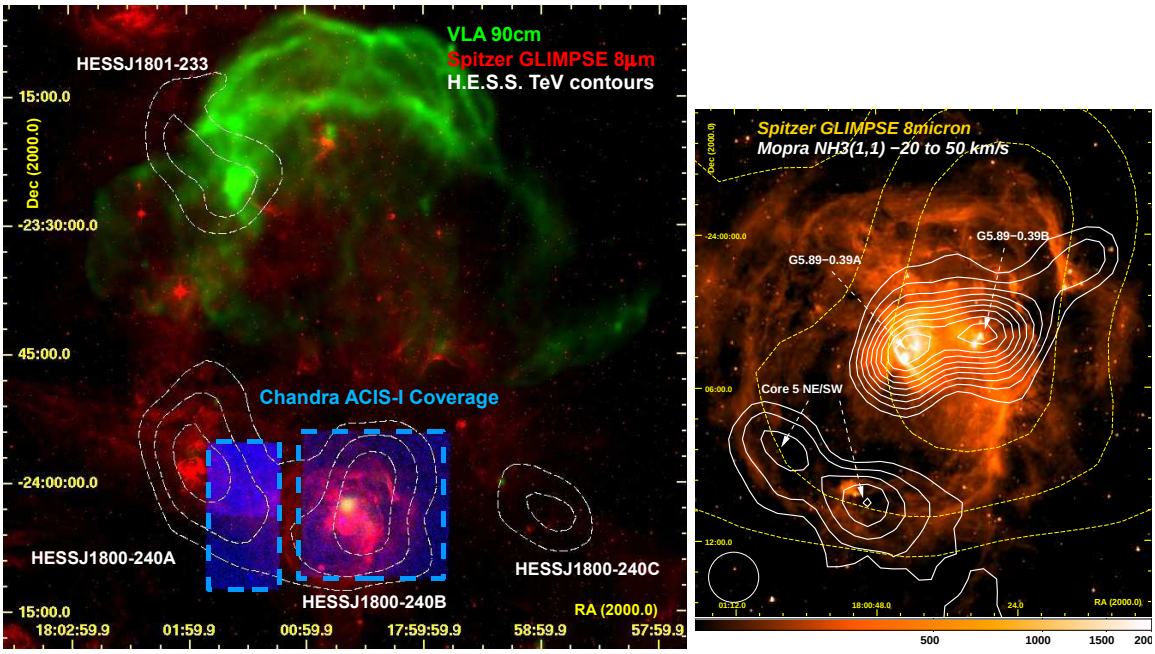

Figure 1: Left: Radio [7] and infrared views of the W28 region with H.E.S.S. 4, 5, and 6σ TeV gamma-ray significance contours (white lines) from [3]. Our *Chandra* ACIS-I coverage towards HESS J1800−240B and G5.89−0.39 is indicated as a blue region with dashed boxes. **Right:** Zoomed in view of the 8μm image (MJy/sr) of HESSJ1800−240B with dense gas contours of $NH_3(1,1)$ from [18]. The $NH_3(1,1)$ peaks can be seen centred on G5.89−0.39A and B. The 10′ wide 8μm ring can also be seen.

2. X-Ray Studies of HII Regions and Status of G5.89−0.39

X-ray studies of HII and UCHII regions are a relatively new activity, and there are open questions concerning the origins of hard X-ray features and outflows seen in the several examples so far [24, 25, 20]. Thermal models are often well-fit albeit with very high temperatures $kT \sim 10$ keV. There is at present no well-understood model for this X-ray emission but the massive protostellar winds with velocities >1000 km s^{-1} expected in these regions may provide a mechanism as discussed earlier. A complication in spectral analyses is the strong low energy X-ray absorption due to the dense molecular gas typically associated with HII regions. Of additional interest here is the search for non-thermal extended or diffuse emission which may arise in the collective effects of stellar winds from a cluster of young massive stars and may reach hard X-ray energies beyond $\sim$8 keV. Such hard diffuse X-ray emission has been observed from a over a dozen massive star formation regions (e.g. M42 [10], Cyg OB2 [13], Westerlund 1 and 2 [16, 17]; see also [19] for a comprehensive list), most of which are also seen at GeV and/or TeV gamma-ray energies.

Most of the X-ray observations in the W28 region have so far been devoted to the SNR shell. The centrally peaked X-ray emission as seen by ROSAT and ASCA [22] is thermal in nature

(*kT* ∼0.4 to 2 keV). A local X-ray peak (or *Ear*) is seen towards the northeastern SNR/molecular cloud interaction, and adjacent to a radio continuum peak which lies within HESS J1801−23. Observations (18 ks) with *XMM-Newton* towards the northeastern region [26] have hinted at weak hard non-thermal component to the X-ray *Ear* emission, but this remains to be confirmed. The ROSAT all sky survey has covered the G5.89−0.39 region with only limited exposure (∼4 ks). The closest catalogued ROSAT source, 1RXS J175938.2−242324, is $\sim 0.5^\circ$ away towards the west.

Our *XMM-Newton* observations (ID50385; ∼27 ks) of G5.89−0.39 and HESS J1800−240B provided the first arcsec resolution X-ray exposure of this HII complex. Unfortunately, strong and steady stray light from the low mass X-ray binary GX 5−1 (∼0.8° to the south) contaminated the *XMM-Newton* MOS and PN detectors, making spectral analyses very difficult.. Nevertheless, several pointlike sources were found, two of which (see Fig. 2) are well-positioned towards G5.89−0.39A and B. In the PN detector at least, these two sources appear to be more distinct against stray light features, and using `SAS v8.0.1 edetect_chain`, we detected them with absorbed fluxes (0.2 to 10 keV) of $\sim 1.0\times10^{-13}$ (G5.89−0.39B) and $\sim 1.4\times10^{-13}$ erg cm^{-2} s^{-1} (G5.89−0.39A). We note that *Suzaku* XIS observations of this region were also taken and will be useful to characterise the large-scale (arcmin) X-ray emission in the region but stray light from GX 5−1 may also affect the *Suzaku* XIS data.

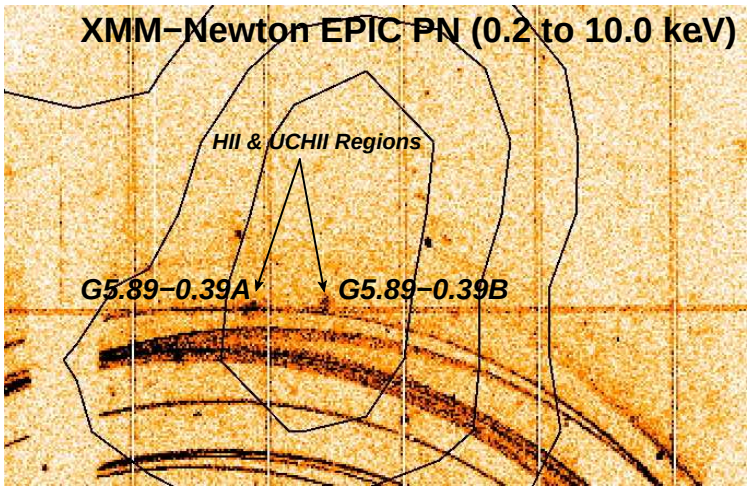

Figure 2: *XMM-Newton* PN image of the G5.89−0.39 region with TeV gamma-ray contours from HESSJ1800−240B indicated by the black solid lines. X-ray sources towards G5.89−0.39A and B can be clearly seen as shown by the black arrows. The stray light streaks contaminate both sources and arise from the low mass X-ray binary GX 5−1 ∼0.8° to the south and just beyond the field of view.

3. G5.89−0.39 *Chandra* Observations and Results

Since *Chandra* is largely unaffected by stray light, it is ideal for very detailed X-ray studies of the G5.89−0.39 region. Our *Chandra* ACIS-I observations (ID10997, 80 ks) were taken over the 30 to 31 July 2010 period. Two of the six ACIS-I chips we configured also covered a part of the neighbouring TeV source HESSJ1800−240A and results from these will be discussed in later work. For processing we used the `CIAO v.4.2.1` and `CALDB v.4.3.0` software and calibration suites. After applying a standard series of event filters (energy interval 0.3 to 10 keV; removal of high flaring total ACIS-I event rate intervals with >20 counts s^{-1}; event rate intervals binned over 200 s outside the 3σ limits of the mean rate), the total dataset amounted to 77.984 ks.

Exposure-corrected maps were generated for the purpose of source detection, and we employed the `wavedetect` algorithm (with default settings) given its improved performance for clustered sources compared to the `celldetect` code.

Fig. 3 shows the full ACIS-I exposure-corrected image. With `wavedetect`, we detected over 200 sources (preliminary) which are encircled with green ellipses/circles. It is clear that many of the sources cluster towards G5.89−0.39A and B and thus our observations may reveal the extent of the associated star formation. Tab. 1 summarises counts and count rates for a selected grouping of sources towards G5.89−0.39A and B which are numbered on Fig. 3. Including these is Feldt's Star [11] (source #66), an O5 or earlier star which may be powering much of the energy in G5.89−0.39B. The slightly offset X-ray emission towards this star may be extended (see Fig. 4) but further analysis is required to confirm this. We find the count rates for our numbered sources are similar to those seen in the young protostellar cluster GGD 27 [20] (which has a similar distance as for G5.89−0.39) and for which the X-ray source luminosities are of order $\sim 10^{31}$ erg s^{-1}, typical of moderate to high mass stars.

Source Number (from `wavedetect`)	Net Counts [counts]	Net Count Rate [counts/cm^2/s]	Source Significance
33	24.5±5.4	$1.1\pm0.3\times10^{-6}$	7.5
44	26.7±6.2	$1.2\pm0.3\times10^{-6}$	6.0
51	33.4±6.8	$1.5\pm0.3\times10^{-6}$	7.2
54	34.8±6.4	$1.8\pm0.3\times10^{-6}$	9.6
55	23.6±5.7	$1.1\pm0.3\times10^{-6}$	5.6
58	16.1±4.4	$0.8\pm0.3\times10^{-6}$	5.5
59	80.5±9.8	$3.7\pm0.5\times10^{-6}$	16.0
62	32.2±6.1	$1.5\pm0.3\times10^{-6}$	9.6
63	20.1±5.2	$0.9\pm0.2\times10^{-6}$	5.3
66 (Feldt's Star)	48.4±8.1	$2.6\pm0.3\times10^{-6}$	9.4
187	16.9±5.2	$0.8\pm0.3\times10^{-6}$	3.9

Table 1: Preliminary X-ray properties (0.3 to 10 keV) of selected *Chandra* sources towards G5.89−0.39A and B detected with the `wavedetect` algorithm. Source numbers are identified in Fig. 3.

4. Conclusions

We have observed with *Chandra* for ∼80 ks, the unusual HII complex G5.89−0.39 towards the centre of the TeV gamma-ray source HESSJ1800−240B. These observations reveal over 200 sources in the ACIS-I field of view, with many sources clustering towards G5.89−0.39A, a HII region, and G5.89−0.39B an ultra-compact HII region. Possibly extended X-ray emission is also seen towards Feldt's Star which may be powering the ultra-compact HII component. Ongoing studies will concentrate on spectral analysis, source cross correlation with other wavebands (e.g. with 2MASS) and the search for extended X-ray emission. Overall, our *Chandra* observations have so far considerably enhanced our understanding of the extent of star formation in the G5.89−0.39 region.

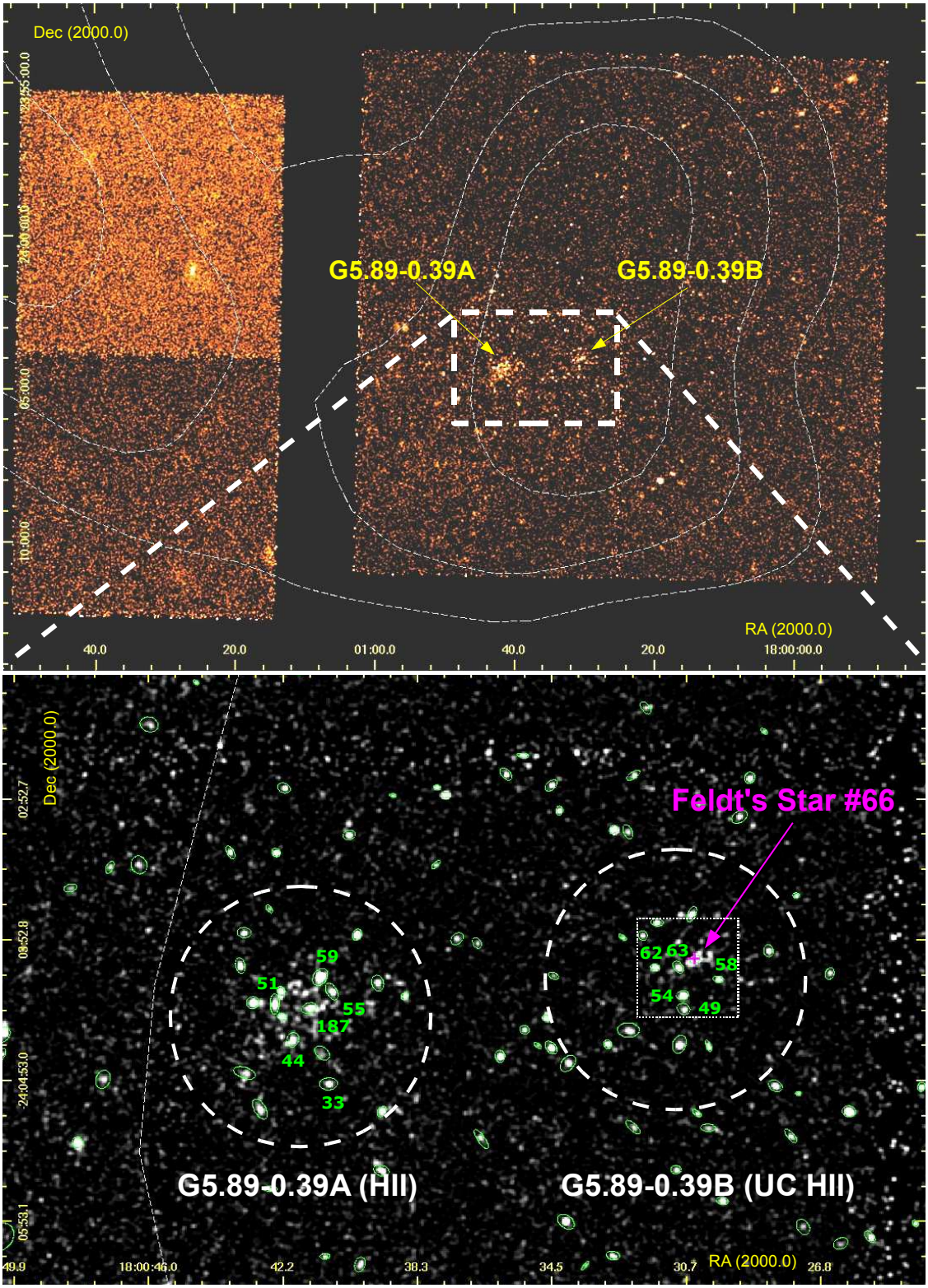

Figure 3: Top: *Chandra* ACIS-I exposure-corrected image (counts $\mathrm{cm}^{-2}\,\mathrm{s}^{-1}$) of the G5.89−0.39 region. White dashed lines represent the TeV gamma-ray contours of HESSJ1800−240B. **Bottom:** Zoom in towards G5.89−0.39A and B components with detected sources encircled by green ellipses/circles. Details for numbered source are given in Tab. 1. The dotted box is the zoom-in of Fig. 4. All images are preliminary.

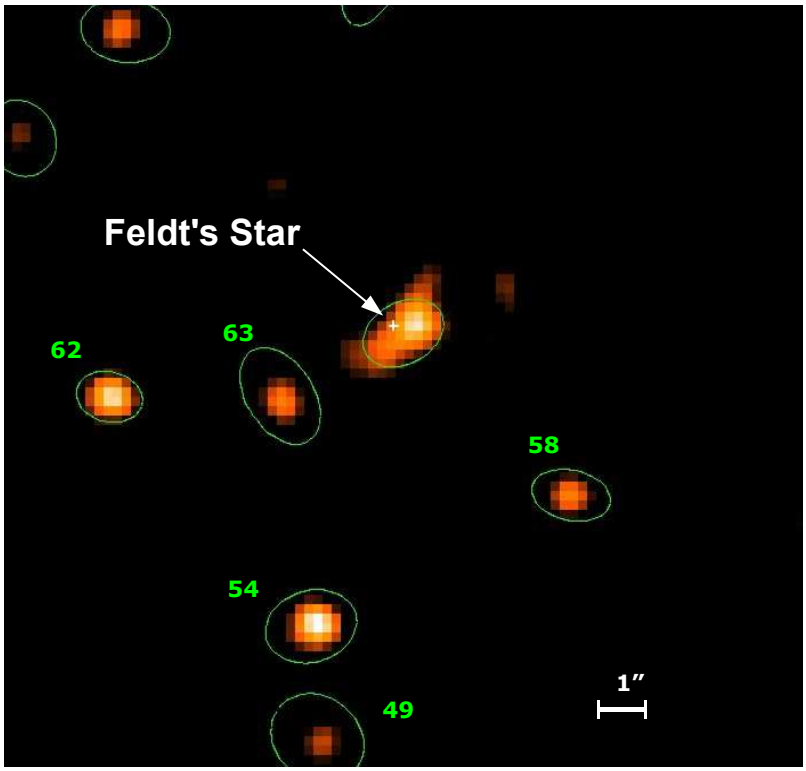

Figure 4: *Chandra* ACIS-I zoom (preliminary) towards Feldt's Star (white cross) within the UCHII region G5.89−0.39B. The size of the white cross depicts the positional error of $\pm 0.2''$ from [11]. Detected X-ray sources are encircled with green ellipses/circles with selected sources numbered as in Fig. 3 and Tab. 1.

References

[1] Acord J. et al. 1997, ApJ, 475, 693.
[2] Aharonian F., et al. (*H.E.S.S. Collab.*) 2006 Nature 439, 695
[3] Aharonian F., et al. (*H.E.S.S. Collab.*), 2008 A&A 481, 401
[4] Araudo A., et al. 2007, A&A, 476, 1289
[5] Arikawa Y., et al., 1999 PASJ 51, L7
[6] Bosch-Ramon V., et al., 2010 A&A 511, A8
[7] Brogan, C. et al, 2006 ApJ 639, L25
[8] Brogan, C. et al. 2008 A&SS 313, 53
[9] Claussen M. J., Frail D.A., Goss W.M., Gaume R.A., 1997, ApJ 489, 143
[10] Ezoe Y., et al. 2006 ApJ 649, L123
[11] Feldt M., et al. 2003 ApJ 599, L91
[12] Harvey P. M., Forveille T., 1988, A&A 197, L19
[13] Horns D., et al. 2007 A&A 469, 17
[14] Kim K., Koo B. 2001, ApJ, 549, 979
[15] Klaassen P.D., Plume R., Ouyed R. et al. 2006 ApJ 648, 1079
[16] Muno M.P. et al. 2006 ApJ 636, L41
[17] Nazé et al. 2009 A&A 483, 171
[18] Nicholas B. et al. 2011 MNRAS 411, 1367
[19] Oskinova L.M. et al. 2010 ApJ 712, 763
[20] Pravdo S. et al. 2009 ApJ 690, 850
[21] Puga E., et al. 2006 ApJ 641, 373
[22] Rho, J., & Borkowsky, K. J., 2002, ApJ 575, 201
[23] Sollins P. K. et al., 2004, ApJ 616, L35
[24] Townsley L.K. et al. 2005 Proc. IAU Symp. 227, 297
[25] Tsujimoto M. et al. 2006 ApJ 653, 409
[26] Ueno M., Bamba A., Koyama K., 2003, Proc. 28th ICRC (Tsukuba, Japan), 2401
[27] Watson C, Churchwell E. et al. 2007 ApJ 657, 318